Electronic Supplementary Material (ESI) for Physical Chemistry Chemical Physics.
This journal is © the Owner Societies 2017

Supplementary Information

Structural formation and charge storage mechanisms for the intercalated two-dimensional carbides MXenes

Jing Wen, Xitian Zhang,* and Hong Gao*

Key Laboratory for Photonic and Electronic Bandgap Materials, Ministry of Education，School of Physics and Electronic Engineering, Harbin Normal University, Harbin 150025, P. R. China

Corresponding author:

Email: xtzhangzhang@hotmail.com; gaohong65cn@126.com

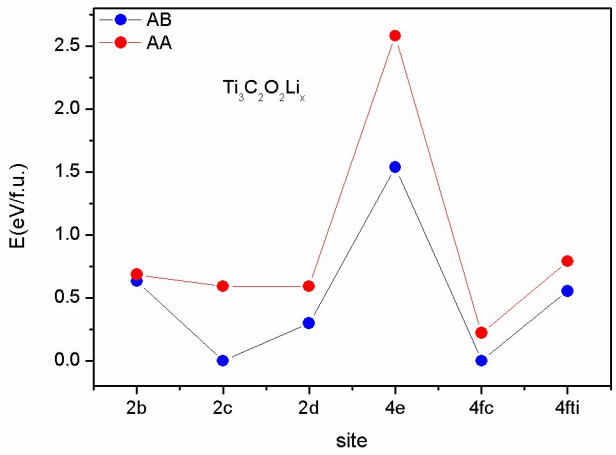

Fig. S1. Energies of $Ti_3C_2O_2Li_x$ as a function of the intercalated site based on the AA and AB configurations. The results are calculated with respect to the minimum values of $Ti_3C_2O_2Li$ and $Ti_3C_2O_2Li_2$, respectively, which correspond to the occupation of Li at the 2*x* (*x=a, b, or c*) and 4*x* (*x=e, fc, or fti*) sites. The symbols are denoted by the Wyckoff letters as 2*b*, 2*c*, 2*d*, 4*e*, 4*fc*, 4*fti*, respectively, where 4*fc* and 4*fti* correspond to the 4*f* positions on the top of C and Ti atoms, respectively.

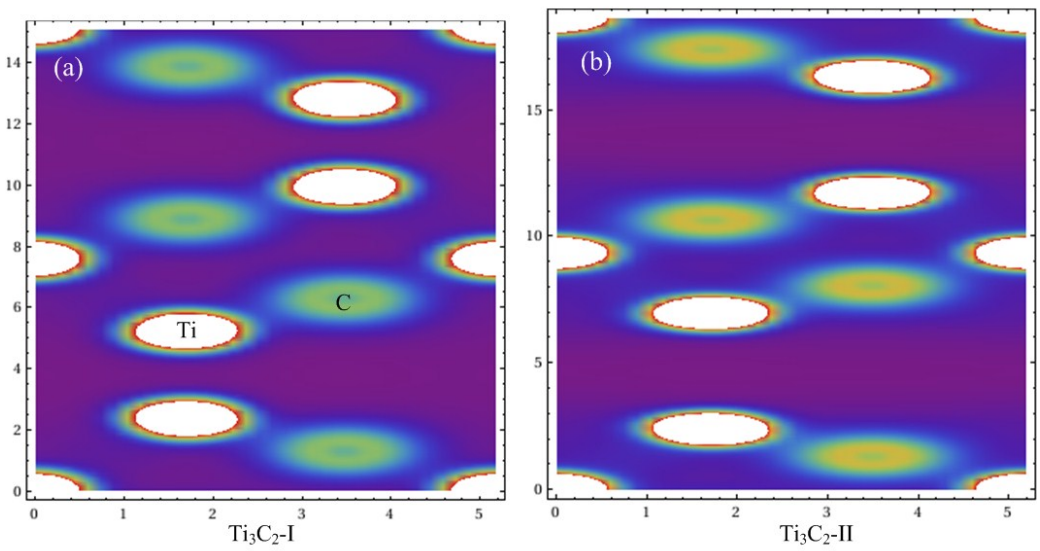

Fig. S2 Charge density distributions of Ti_3C_2 projected in the (110) sections with *c*-axis values of 15.18 Å (a) and 18.68 Å (b), respectively. The intensities are gradually decreased from red to purple. It is obvious that the metallic bonding in the interlayer

spaces of Ti_3C_2 can be comparable to that in the Ti_3C_2 slabs when its *c*-axis value is contracted to about 15 Å (Fig. S2(a)). It gradually decreases with the increasing interlayer distance (Fig. S2(b)).

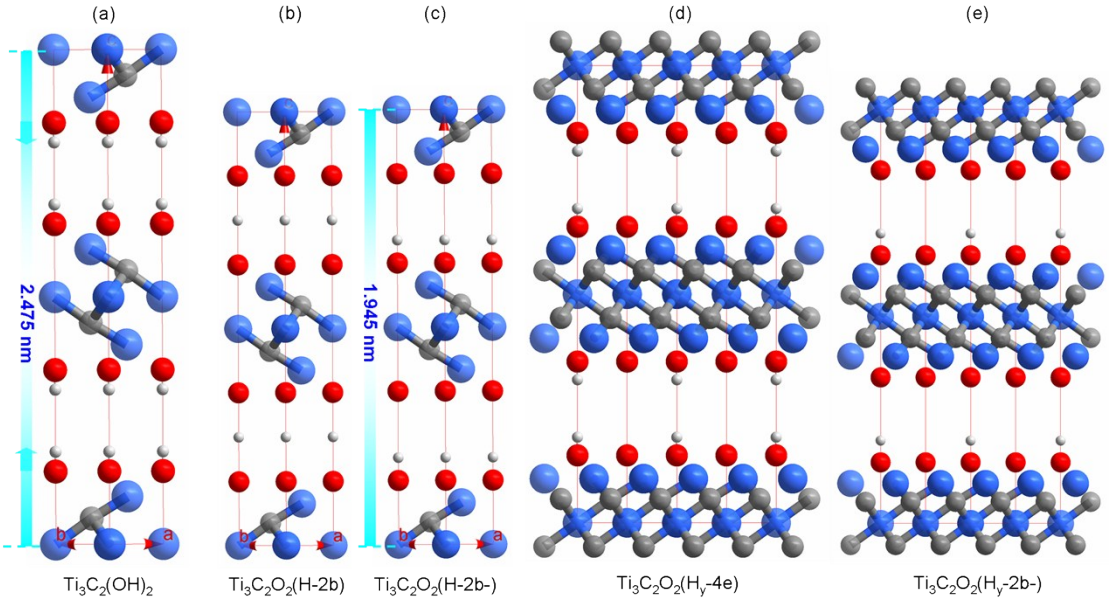

Fig. S3. Structural models of $Ti_3C_2O_2H_y$ with H occupy the 4*e* site (a), 2*b* site (b), 2*b*-site (c), partial 4*e* sites (d), and partial 2*b*- sites (e), respectively. The c-axis values of $Ti_3C_2(OH)_2$ and $Ti_3C_2O_2$(H-2*b*-) are obtained from their optimized structures.

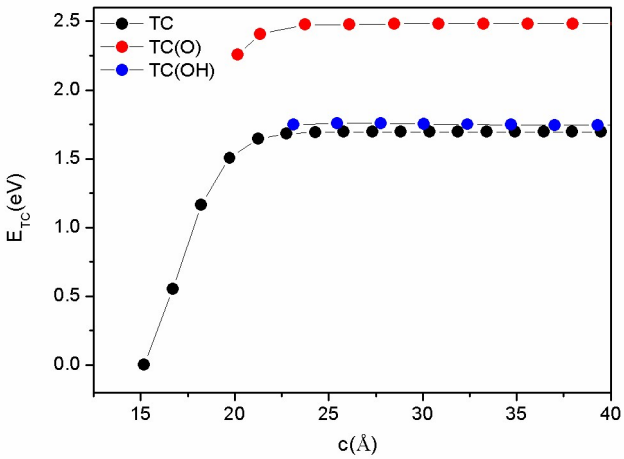

Fig. S4. Energies of Ti_3C_2 (denoted by E_{TC}) transformed by the intercalated -O and -OH groups and that of pristine Ti_3C_2 as the functions of *c*-axis values.

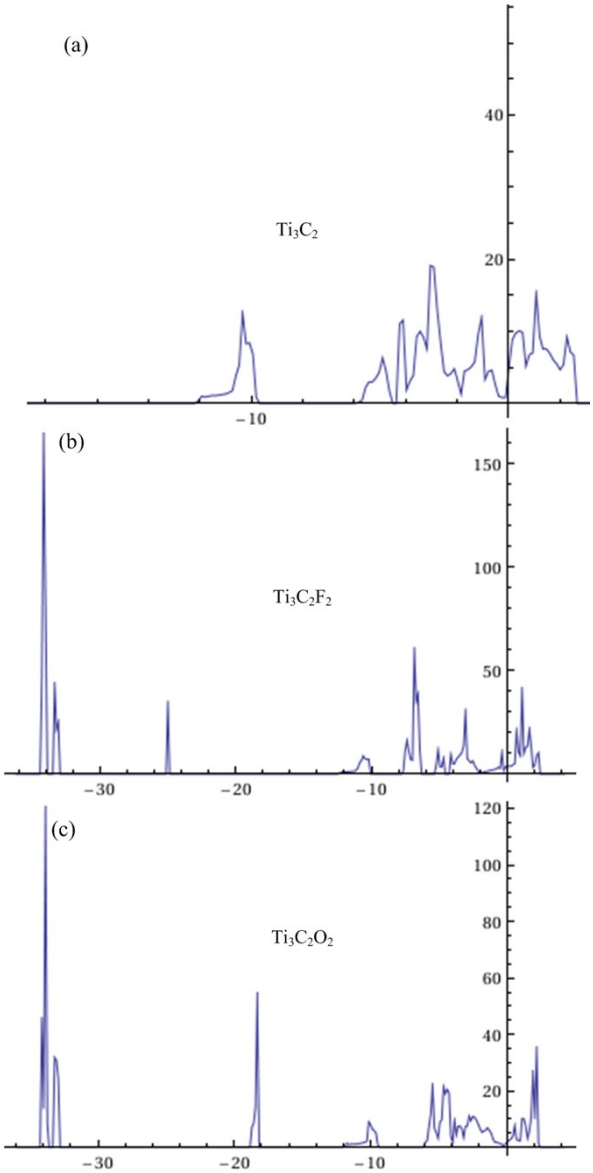

Fig. S5. The densities of states (DOS) of Ti_3C_2 (a), $Ti_3C_2F_2$ (b), and $Ti_3C_2O_2$ (c). It is clear that the conduction property vary with the type of surface structure. It changes from mental to semiconductor after the surface of pristine Ti_3C_2 forming the coordination structures $Ti_3C_2F_2$ and $Ti_3C_2O_2$.

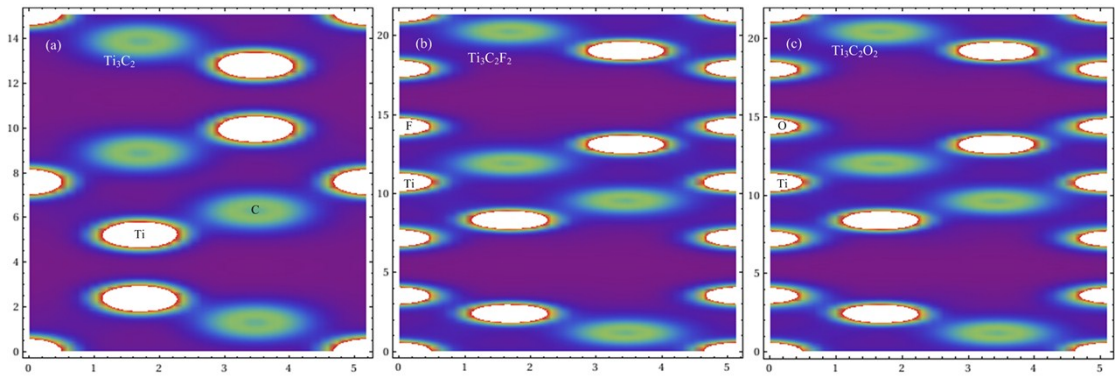

Fig. S6. Charge density distributions of Ti_3C_2 projected in the (110) sections (a) and that of $Ti_3C_2F_2$ (b), and $Ti_3C_2O_2$ (c). The intensities are gradually decreased from red to purple.

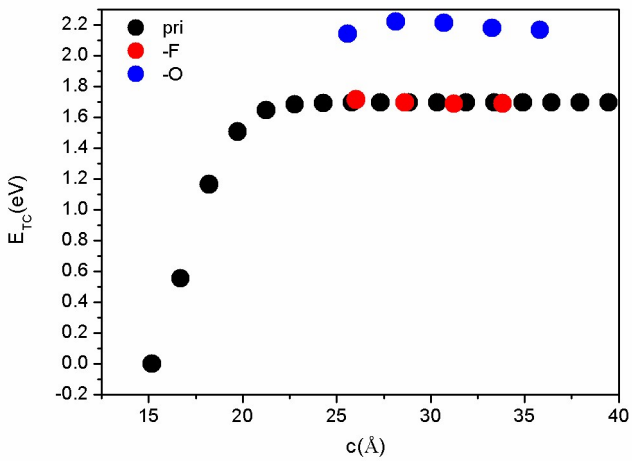

Fig. S7. Calculated energies of Ti_3C_2 based on the structure of pristine Ti_3C_2 with expanded *c*-axis value (denoted by pri), and that based on the structure formed by taking away the Li and F (O) elements from the $Ti_3C_2F_2Li_2$ ($Ti_3C_2O_2Li_2$) configurations (denoted by –F (-O)). The classification of the charge storage mechanism is based on the calculated energies of Ti_3C_2. The energy of pristine Ti_3C_2 is consistent with that of the structure denoted by -F. According to the Hohenberg-Kohn theorems, it means that the electron density nearly remain unchanged after the Li element being introduced into the host, so it can be deduced that the physical adsorption is the dominant charge storage process for the $Ti_3C_2F_2$ unit cell. In contrast, the $Ti_3C_2O_2$ unit cell satisfies the chemical adsorption conditions due to the

redistribution of the charge density in the host, so the charge storage mechanism should be the redox process.